MOSAICING WITH THE BIMA ARRAY

Tamara T. Helfer

Radio Astronomy Laboratory, 601 Campbell Hall, UC Berkeley, Berkeley, CA 94720 USA
thelfer@astro.berkeley.edu

ABSTRACT

Mosaicing is now a routine mode of observing at the 10-element Berkeley-Illinois-Maryland Association (BIMA) millimeter interferometer and has produced results not previously possible with millimeter-wavelength observations. In this paper, I describe imaging simulations of mosaiced observations at BIMA and other millimeter telescopes that illustrate the issue of the attenuation of flux from large structures on the sky caused by the spatial filtering property of an interferometer, and I compare these simulations to real observations. I also describe recent mosaicing projects at BIMA, with particular attention to the issue of adding single-dish data to mosaiced observations.

IMAGING SIMULATIONS OF LARGE-SCALE FLUX RECOVERY AT MILLIMETER WAVELENGTHS

The recovery of large-scale flux is a serious problem for millimeter-wavelength interferometers, since telescopes routinely resolve out flux on size scales that are relevant to the science. At the Berkeley-Illinois-Maryland Association (BIMA) millimeter interferometer, each of the primary dishes of the interferometer is 6 m in diameter, so that the primary field of view is about $100''$ FWHM at 3 mm wavelength. Mosaicing is therefore required to image sources on the sky larger than about an arcminute. Multiple-field imaging simulations at mm wavelengths [1] demonstrate the advantages of mosaicing. First, the nonlinear deconvolutions routinely applied to interferometric maps interpolate and extrapolate to unsampled spatial frequencies and thereby reconstruct much larger scale structures than an analytical treatment of the flux recovery issue would suggest. Second, the simulations demonstrate an extension of the Ekers and Rots [2] effect, namely, that how well an individual telescope recovers large-scale structure for a mosaiced observation is more closely related to the minimum distance between its dishes, $S_{min} - D$, than to the minimum center-to-center distance, S_{min}. The simulations also show that the fraction of flux recovered for a given observation is a function of the signal-to-noise ratio of the map (Fig. 1). Both noise-free and noise-added simulations demonstrate that, in order to make accurate high-resolution maps of even moderately large ($>20''$) sources at millimeter wavelengths, it is generally necessary to include single-dish ("total power") or very short uv-spacing data. For a source that is large in one dimension but small in another (e.g. an elliptical Gaussian), the simulations show that as long as the small dimension is small enough, the deconvolution can recover the flux even in the long dimension. This may help with the real imaging of spiral galaxies, where the rotation tends to confine the emission in any given channel map to a relatively small region in one dimension.

SAMPLING REQUIREMENTS AND OBSERVING TECHNIQUES

Multiple-pointing observations require fast switching among the fields, so that the uv plane can be sampled as completely as possible. At 3 mm, the time needed to cross an individual cell Δu in the uv plane for a mosaiced observation of a source of size θ_s is $t_{\Delta u} \approx 160\ (\theta_r/\theta_s)$ minutes, where θ_r is the resolution of the observations [1]. Given a nominal source size of $60''$, the limiting time to cross an individual cell at $5''$ resolution is about 13 minutes. This means that, for these parameters, an individual field should be observed every 13 minutes or less. At BIMA, mosaics are routinely carried out with integration times of 1 minute or less per pointing, as the project requires. In practice, switching fields every minute or less without losing a significant amount of time to overhead means that the telescope must be designed to handle fast data dump times and to have fast settling times for the array elements. Good sampling requirements also dictate that there is a practical limit on the number of fields that can be observed in one track. Since large dishes require correspondingly more pointings to cover the same region of the sky than small dishes, they may be at somewhat of a disadvantage for obtaining good sampling over large regions.

BIMA MOSAICS

Mosaicing small numbers of fields is a routine mode of observing at BIMA, and the observing setup and data reduction software are flexible and easy to use. Approximately one quarter of recent proposals for all configurations at BIMA requested mosaiced observations. Here, I describe some of the recent results of some multiple-pointing projects.

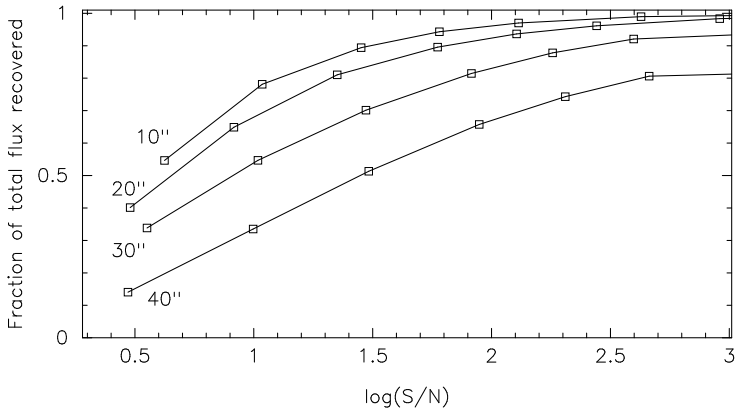

Figure 1: Fraction of total flux recovered inside a $\pm 100''$ box for BIMA simulations of spiral models as a function of the log of the signal-to-noise ratio. Simulations are shown for spiral models with arms widths of 10, 20, 30, and $40''$. The plots reflect the fact that it is increasingly difficult for the deconvolution to reconstruct large-scale flux as the signal-to-noise ratio decreases. Figure and caption are adapted from [1].

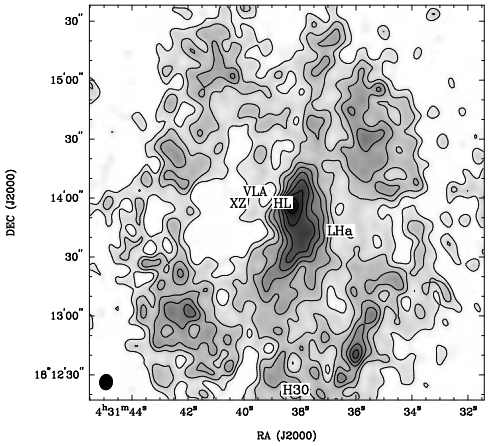

Figure 2: Mosaiced ^{13}CO BIMA+12m integrated intensity map of the environs around XZ Tau and HL Tau. While the flux density is strongest near HL Tau, the overall structure suggests a ring or bubble centered to the east of HL Tau, near XZ Tau. Figure is taken from [3].

Wide-Field Imaging of the HL Tauri Environment in ^{13}CO

In practice, mosaicing large fields and adding single-dish data can have a dramatic impact on the interpretation of an interferometric map. For example, Welch et al. [3] recently presented a 7-field mosaiced BIMA plus NRAO 12m single dish map of ^{13}CO J = 1–0 emission from the region surrounding and including the pre-main-sequence star HL Tau (Fig. 2). This image showed for the first time the result that structures on size scales of $>$1000 AU are not a large-scale protostellar disk associated with HL Tau itself but are instead part of a much larger (20000 AU, or 0.08 pc) shell centered on its neighbor, XZ Tau.

Giant Molecular Clouds in the Optical Disk of M33

Another recent mosaicing project at BIMA involved mapping and cataloging the CO J = 1–0 emission from Giant Molecular Clouds (GMCs) in the nearby galaxy M33 [4]. The M33 mosaic comprised 759 pointings and covered almost the entirety of the optical galaxy (Fig. 3); the data were used to produce the first complete catalog of GMCs in any spiral galaxy (including the Milky Way). The molecular emission is very sparse but it closely follows the features seen in atomic hydrogen. Preliminary results from follow-up BIMA observations at higher resolution show that the the clouds have an angular momentum deficit of one to two orders of magnitude under the assumption that they condensed from the atomic gas. This suggests that the clouds are braked by magnetic fields that tie the clouds to the ambient medium. Surprisingly,

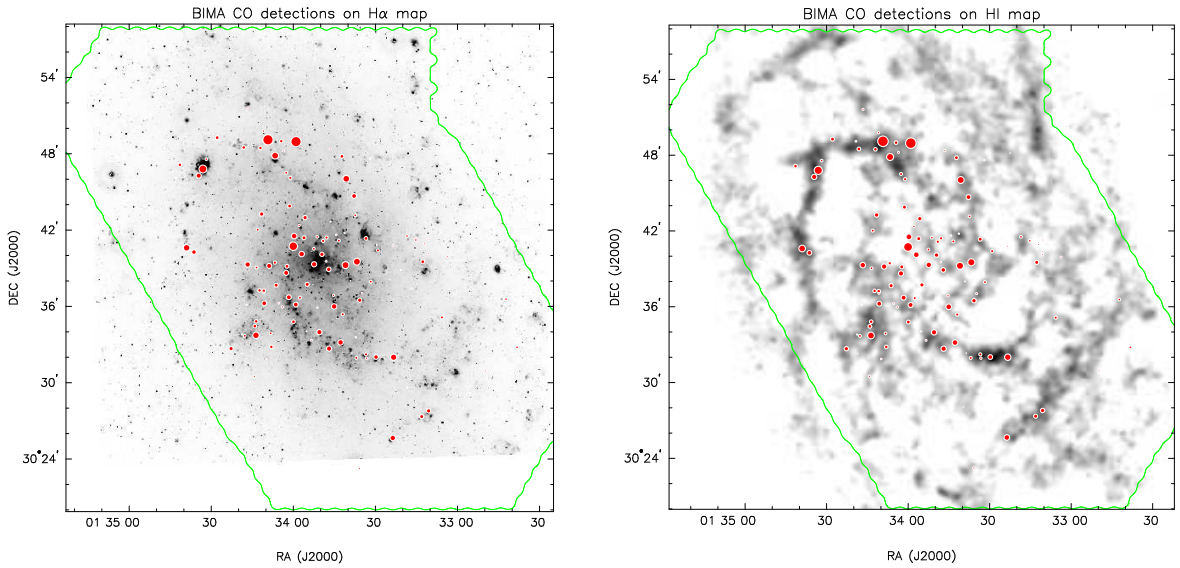

Figure 3: Giant Molecular Clouds in M33 [4]. The most significant BIMA CO cloud detections are shown as red dots and are overlaid on an Hα image (left) [7] and on a clipped, integrated intensity map of the HI emission (right) [8]. The area of each red dot is proportional to the cloud mass; masses range from 1×10^4 $M_\odot$ to 7×10^5 $M_\odot$. The outer green contour indicates the limits of the BIMA mosaic, which required 759 telescope pointings.

the most massive cloud has no HII region, and would thus have been difficult to find using search strategies employed either by single dishes or non-mosaiced observations.

The BIMA Survey of Nearby Galaxies (BIMA SONG)

The BIMA Survey of Nearby Galaxies (SONG) [5,6] is the first systematic imaging survey of the CO emission within the centers and disks of 44 nearby spiral galaxies. Mosaiced observations were obtained for the largest two-thirds of the sample, and single-dish On-the-Fly data from the NRAO 12 m telescope were also incorporated into 24 of the BIMA SONG maps.

Sample BIMA SONG data for a combined, BIMA+12m 26-field mosaic of NGC5194 (M51) are shown in Fig. 4. At left is the integrated intensity map, made using a mask-and-clip technique, which is very effective at showing low-level emission which is distributed in a similar way to the brighter emission in the map. (Such low-level distributions are common, since the deconvolution typically leave systematic, positive residuals in the shape of the source, which is almost certainly true emission associated with the source.) The flux recovery data for NGC5194 are illustrated in the middle and right panels of Fig. 4. The middle panel shows a pixel-by-pixel flux recovery ratio map of the BIMA-only data, smoothed to $55''$ resolution, compared with the $55''$-resolution of the 12m data. Just over 80% of the total single-dish flux density is recovered over the brightest regions of the source, and the ratio falls off away from the galaxy center as a function of the brightness of the emission. The dependence of the flux recovery on the signal-to-noise (S/N) ratio of the interferometer data, predicted by simulations and shown in Fig. 1, is readily apparent in real data, as shown in the right panel of Fig. 4.

The trend seen in the NGC5194 map is generally seen in other BIMA SONG data as well. There is typically a large region near the center (or near the brightest emission, which is often in the center) where the flux density recovered is highest, and the ratio of flux recovered falls as a function of distance from the center (where the emission tends to be weaker). This trend may be attributed to two factors: first, for any given velocity in a data cube, there is a larger region of sky available to emit at locations away from the center of the galaxy rather than at the center (that is, the velocity gradient is largest at the nucleus). Second, the tendency is for the brightest emission and best sensitivity to be near the center, so that the S/N ratio is highest in the central region. From Figs. 1 and 4, we expect the deconvolution to reconstruct less of the total flux in regions of lower S/N.

For NGC5194 and the other 23 BIMA SONG galaxies with OTF data, we have of course incorporated the 12 m OTF data in the BIMA SONG maps so that the total flux is accurate for these maps. Furthermore, structures larger than $55''$ should be accurately represented in the BIMA+12 m SONG maps, and structures $\lesssim 20''$ should also be accurately

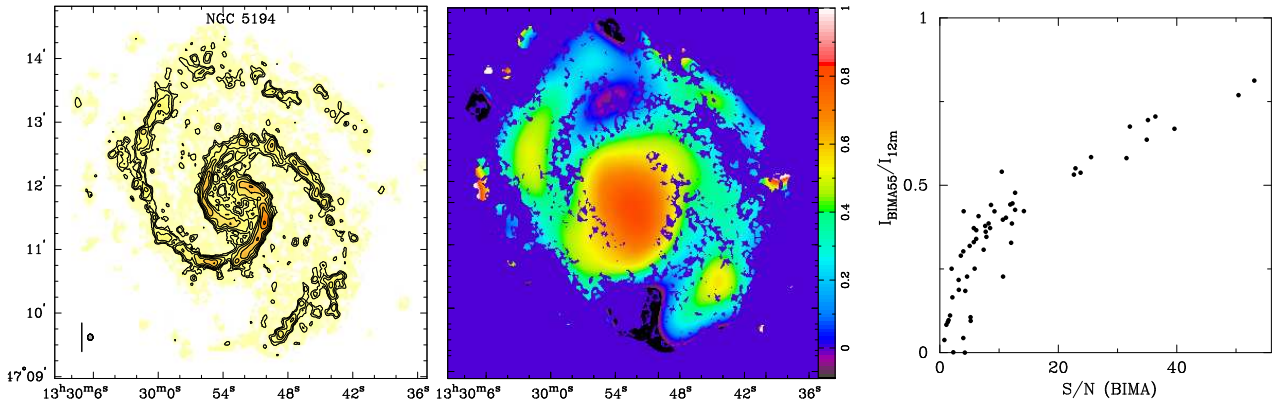

Figure 4: BIMA SONG CO data for NGC5194 (M51). The mosaic includes 26 fields. **Left:** BIMA+12m CO contours (spaced by 1.59 times the previous interval) overlaid on a false-color representation of the same image. The $5.8'' \times 5.1''$ FWHM of the synthesized beam is shown near the lower left corner of the box, next to a vertical bar that shows the angular size of 1 kpc at the assumed distance (7.7 Mpc) to the source. **Middle:** Flux recovery ratio map. The scale is shown as a wedge to the right. **Right:** Ratio of flux recovered as a function of S/N in the BIMA-only data, smoothed to $55''$. Figure adapted from [6].

represented in the maps. It is difficult to be confident of the accuracy of structures on the intermediate size scales of $20–55''$. In all likelihood, these structures are somewhat misrepresented as their attenuated BIMA-only structures sitting atop a smoothed-out 12 m plateau.

REFERENCES

[1] T. T. Helfer, S. N. Vogel, J. B. Lugten, and P. J. Teuben, "Imaging Simulations of Large-Scale Flux Recovery at Millimeter Wavelengths", *Publications of the Astronomical Society of the Pacific*, vol. 114, p. 350, 2002.

[2] R. D. Ekers and A. H. Rots, "Short Spacing Synthesis from a Primary Beam Scanned Interferometer", in *Image Formation from Coherence Functions in Astronomy*, C. van Schooneveld, Ed., ASSL vol. 76, p. 61, 1979.

[3] W. J. Welch, L. Hartmann, T. Helfer, and C. Briceño, "High-Resolution, Wide-Field Imaging of the HL Tauri Environment in ^{13}CO (1-0)", *Astrophysical Journal*, vol. 540, p. 362, 2000.

[4] G. Engargiola, R. L. Plambeck, E. Rosolowsky, and L. Blitz, "The BIMA Survey of Giant Molecular Clouds in the Optical Disk of M 33", in preparation.

[5] M. W. Regan, M. D. Thornley, T. T. Helfer, K. Sheth, T. Wong, S. N. Vogel, L. Blitz, and D. C.-J. Bock, "The BIMA Survey of Nearby Galaxies. I. The Radial Distribution of CO Emission in Spiral Galaxies", *Astrophysical Journal*, vol. 561, p. 218, 2001.

[6] T. T. Helfer, M. D. Thornley, M. W. Regan, T. Wong, K. Sheth, S. N. Vogel, L. Blitz, and D. C.-J. Bock, "The BIMA Survey of Nearby Galaxies. II. The CO Data", submitted.

[7] K. P. Cheng, P. Hintzen, E. P. Smith, R. Angione, F. Talbert, N. Collins, and T. Stecher, "Ground-Based CCD Images in Support of the Astro-1/UIT Space Shuttle Mission on CD-ROM", *American Astronomical Society Meeting*, vol. 188, p. 5403, 1996.

[8] E. R. Deul and J. M. van der Hulst, "A survey of the neutral atomic hydrogen in M33", *Astronomy and Astrophysics Supplement Series*, vol. 67, p. 509, 1987.